DALTON

Metal(II) N_2S_2 Schiff-base complexes incorporating pyrazole or isoxazole (M = Ni, Cu or Zn). Spin states, racemization kinetics and electrochemistry †

Agnete la Cour,*[a] Matthias Findeisen,[b] Alan Hazell,[c] Rita Hazell[c] and Grit Zdobinsky[b]

[a] *Department of Chemistry, Odense University, DK-5230 Odense M, Denmark*
[b] *Department of Analytical Chemistry, Leipzig University, Liebig Strasse, D-04103 Leipzig, Germany*
[c] *Department of Chemistry, Aarhus University, DK-8000 Århus C, Denmark*

Schiff-base complexes incorporating a five-membered aromatic heterocycle (isoxazole or pyrazole) and biologically important 3d metal(II) ions (M = Ni, Cu or Zn) have been synthesized. The crystal structures have been determined for [*N*,*N*′-bis(3-phenyl-5-sulfanylisoxazol-4-ylmethylene)butane-1,4-diaminato]copper(II) **1b** and for [*N*,*N*′-bis(1-methyl-3-phenyl-5-sulfanylpyrazol-4-ylmethylene)butane-1,4-diaminato]nickel(II) **2a**. In both structures the metal atom is co-ordinated to two nitrogen and to two sulfur atoms which form a flattened tetrahedron with the dihedral angles between the two N–M–S planes being 48.6(1) and 12.7(1)° respectively. Their physicochemical properties have been studied in solution. The spin-equilibrium process $S = 0 \rightleftharpoons S = 1$ and the racemization process $\Delta \rightleftharpoons \Lambda$ for the nickel(II) complexes have been investigated by temperature-dependent ^{1}H NMR spectroscopy. Complex **2a** (ΔG = 7.8 kJ mol^{-1} at 25 °C) is more stabilized in the low-spin state than is **1a** (ΔG = 3.2 kJ mol^{-1}). The racemization rates are 2.3 × 10^4 and 1.7 × 10^4 s^{-1} at 25 °C for **1a** and **2a**, respectively. The stereochemistry of the zinc(II) and copper(II) complexes in solution seems to be independent of the ligand. For the former the configurations were evaluated from the chemical shift differences between diastereotopic protons. For the latter structural similarities are seen in the electronic and ESR spectra. The electrochemical properties have been investigated by cyclic voltammetry. The isoxazole ligand stabilizes a high potential for the M^{II}–M^{I} reduction ($E_{\frac{1}{2}} \approx 0$ for Cu) compared with the pyrazole ligand ($E_{\frac{1}{2}} = -407$ mV for Cu).

Nickel, copper and zinc are important metals in the chemistry of life. Among the more investigated metalloenzymes are nickel hydrogenase, the copper-containing cytochrome c oxidase, azurin and plastocyanin, and the zinc-containing alcohol dehydrogenase. The crystal structures of the metal centres have been solved.[1] These enzymes are all involved in redox chemistry in cellular life, and they are all totally or partly ligated by sulfur donor atoms in the active site of the enzymes.

It is the purpose of our work to find biologically interesting effects of ligand modifications on the physicochemical properties of transition-metal complexes. For that reason we have synthesized the sulfur-containing Schiff-base complexes **1** and **2**.

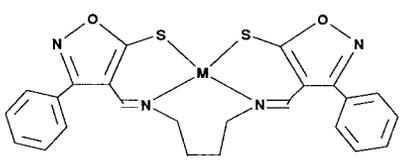

[ML^1]

M

1a Ni
1b Cu
1c Zn

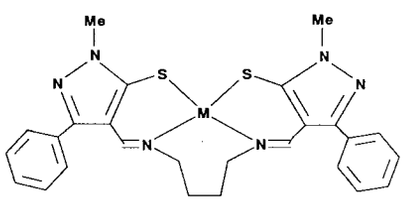

[ML^2]

M

2a Ni
2b Cu
2c Zn

Results and Discussion

Syntheses and identification

Yields and analytical data are presented in Table 1. The tetranuclear copper(I) complex **2b**′ is easily obtained from the reaction of copper(II) acetate and H_2L^2 added in the ratio 2:1. It was identified from the FAB mass spectrum in $CHCl_3$ which proves that it is stable in solution. According to the elemental analyses and the FAB mass spectrum, **2b** contains small amounts of the copper(I) complex. Tetranuclear copper(I) complexes with tetradentate ligands similar to H_2L^2 have been obtained recently.[2] The crystal structure determination of one complex shows that the surroundings of the copper(I) ions are pseudo-tetrahedral.[2]

Crystal structures

Crystal data are listed in Table 2, selected bond distances and angles in Tables 3 (**1b**) and 4 (**2a**). Both structures contain discrete molecules without special intermolecular interactions. Complex **1b** (Fig. 1) lies on a crystallographic two-fold axis and therefore has exact two-fold symmetry. The copper atom is co-ordinated to two nitrogen and to two sulfur atoms which form a flattened tetrahedron with Cu–N 1.927(3), Cu–S 2.260(1) and S···S 3.138(3) Å. The dihedral angle, θ, between the N–Cu–S planes is 48.6(1)°. Complex **2a** (Fig. 2) has approximate two-fold symmetry. The nickel atom is co-ordinated to two nitrogen

† *Supplementary data available* (No. SUP 57187, 4 pp.): spin equilibrium, coupling and rate constants and NMR data. See Instructions for Authors, *J. Chem. Soc., Dalton Trans.*, 1997, Issue 1.
Non-SI units employed: G = 10^{-4} T, $\mu_B \approx 9.27 \times 10^{-24}$ J T^{-1}.

Table 1 Solvents for recrystallization, yields and analytical data

Complex	Recrystallized from	Yield[a] (%)	Analysis (%) C	H	N	EI mass spectrum, *m/z*[c]
1a	CH_2Cl_2	51 (35)[d]	55.65 (55.5)	3.95 (3.90)	10.85 (10.8)	518
2a·0.1$CHCl_3$	$CHCl_3$	53 (43)[d]	56.85 (56.25)	4.90 (4.70)	14.85 (15.1)	544
1b	*e*	55	54.5 (55.0)	3.70 (3.85)	10.2 (10.7)	523
2b	—	80	55.15 (56.75)	5.05 (4.75)	14.35 (15.3)	551[f] (M^+ + 2)
2b′[g]	—	85	50.1 (50.9)	4.40 (4.25)	13.5 (13.7)	1226[f] (M^+ + 2)
1c	—	68	54.45 (54.8)	3.80 (3.85)	11.35 (10.65)	524
2c·2H_2O	—	70	52.65 (53.1)	4.55 (4.80)	14.15 (14.3)	550

[a] From protonated pro-ligand. [b] Calculated values in parentheses. [c] The molecular ion, M^+ (crystal solvent not included). [d] Yield of protonated pro-ligand (from *o*-chloroaldehyde). [e] Not recrystallized. [f] FAB mass spectra. The tetranuclear complex is also seen in the spectrum of **2b**. [g] Composition: 4 Cu^I and two ligands.

Table 2 Crystal data and details of data collection and structure refinement for complexes **1b** and **2a**[a]

	1b	**2a**
Formula	$C_{24}H_{20}CuN_4O_2S_2$	$C_{26}H_{26}N_6NiS_2$
M	524.11	545.8
Crystal system	Orthorhombic	Monoclinic
Space group	*Pbcn*	$P2_1/c$
a/Å	8.096(2)	8.5137(7)
b/Å	14.149(3)	11.4185(8)
c/Å	20.399(5)	26.216(2)
β/°	90.0	91.926(5)
U/Å^3	2337(1)	2547.1(3)
Z	4	4
Crystal size/mm	0.44 × 0.36 × 0.09	0.55 × 0.30 × 0.15
D_c/ cm^{-3}	1.490	1.422
F(000)	1076	1136
μ/cm^{-1}	11.355	9.475
Absorption correction range	0.923–1.165	0.759–0.870
2θ range/°	2–50	2–60
hkl Range	0, 0, 0 to 9, 16, 24	−11, 0, 0 to 11, 15, 36
Decay (%)	5	1
Unique data	2038	7460
Observed data [$I/\sigma(I) > 3$], N_o	1264	4714
Variables, N_v	190	421
R	0.033	0.038
R′	0.041	0.051
S	1.056	1.168
$(\Delta/\sigma)_{max}$	0.005	0.129
$\Delta\rho_{max}$, $\Delta\rho_{min}$/e Å^{-3}	0.27(5), −0.29(5)	0.42(6), −0.28(6)

[a] $R = \Sigma(|F_o| - |F_c|)/\Sigma|F_o|$, $R' = [\Sigma w(|F_o| - |F_c|)^2/\Sigma w|F_o|^2]^{\frac{1}{2}}$, $S = \Sigma w(|F_o| - |F_c|)^2/(N_o - N_v)$. Weighting scheme: $1/w = [\sigma(F)^2 + 1.03F^2]^{\frac{1}{2}} - |F|$, refinement based on *F*. S.e.s of the least significant digits are in parentheses.

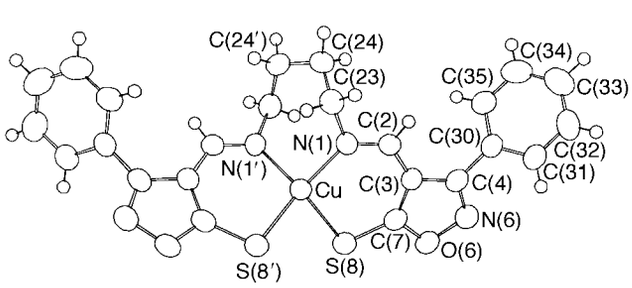

Fig. 1 Molecular structure of complex **1b**

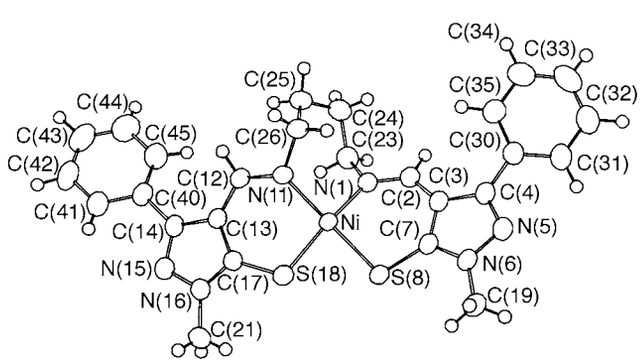

Fig. 2 Molecular structure of complex **2a**

and to two sulfur atoms which form a very flattened tetrahedron [θ = 12.7(1)°] with Ni–N 1.932(2) and 1.935(2), Ni–S 2.196(1) and 2.187(1) and S···S 2.858(1) Å.

The different co-ordination geometries of the two structures are mainly attributed to the different metal atoms. The geometry of **1b** is similar to other copper(II) N_2S_2 Schiff-base complexes with tetradentate ligands bridged by four ($n = 4$) carbon atoms (θ ≈ 50°).[3a,c,d] The co-ordination tends to be more planar for the analogous nickel(II) complexes.[4] Some variations

Table 3 Selected bond distances (Å) and angles (°) for complex **1b**

Cu–N(1)	1.927(3)	Cu–S(8)	2.260(1)
N(1)–C(2)	1.291(4)	N(1)–C(23)	1.489(5)
C(2)–C(3)	1.419(5)	C(3)–C(4)	1.431(5)
C(3)–C(7)	1.375(5)	C(4)–N(5)	1.295(5)
C(4)–C(30)	1.477(5)	N(5)–O(6)	1.435(4)
O(6)–C(7)	1.346(4)	C(7)–S(8)	1.704(4)
C(23)–C(24)	1.503(6)	C(24)–C(24′)	1.525(9)
S(8)···S(8′)	3.138(3)		
N(1)–Cu–N(1′)	93.9(2)	S(8)–Cu–S(8′)	87.92(7)
N(1)–Cu–S(8)	100.7(1)	N(1)–Cu–S(8′)	142.9(1)
Cu–N(1)–C(2)	128.2(3)	Cu–N(1)–C(23)	117.7(2)
C(2)–N(1)–C(23)	114.0(3)	N(1)–C(2)–C(3)	126.0(4)
C(2)–C(3)–C(7)	128.5(4)	C(4)–C(3)–C(7)	103.4(3)
C(2)–C(3)–C(4)	127.9(4)	C(3)–C(4)–N(5)	112.9(4)
C(4)–N(5)–O(6)	105.4(3)	N(5)–O(6)–C(7)	108.4(3)
C(3)–C(7)–O(6)	110.1(3)	O(6)–C(7)–S(8)	117.5(3)
C(3)–C(7)–S(8)	132.4(3)	Cu–S(8)–C(7)	103.3(1)
N(1)–C(23)–C(24)	113.9(4)	C(23)–C(24)–C(24′)	116.5(3)
C(31)–C(30)–C(35)	118.3(4)	C(4)–C(30)–C(31)	119.8(4)
N(1)–Cu–S(8)C S(8′)–Cu–N(1′)	48.6(1)		
C(3)–C(4)–C(30)–C(31)	129.8(5)	N(5)–C(4)–C(30)–C(31)	−49.0(6)
C(3)–C(4)–C(30)–C(35)	−52.0(7)	N(5)–C(4)–C(30)–C(35)	129.2(5)

E.s.d.s of the least significant digits are in parentheses.

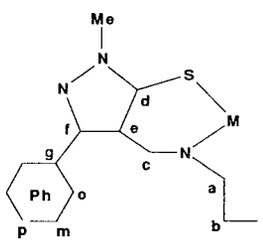

Scheme 1 Numbering scheme for the assignments of NMR spectra for compounds **2**. The methyl signal is missing for compounds **1**

due to the different heterocycles are supposed to be independent of the metal ion. The less aromatic character expected,[5] and actually found for the isoxazole compared with the pyrazole ring, is also reflected in the chelate rings. According to the bond distances, the electron density is most delocalized in **2a**. The higher degree of conjugation between the phenyl substituent and the heteroaromatic ring observed for **2a** may also be a result of the greater aromatic character of the pyrazole ring: the torsion angle C(3)–C(4)–C(30)–C(35), is −52.0(7) and 23.9(5)° for **1b** and **2a**, respectively (see Tables 3 and 4).

The M–L bond lengths are significantly different from those reported for a series (n = 2–4) of metal(II) N_2S_2 Schiff-base complexes with an incorporated carbon ring, *i.e.* cyclopentene.[3a,b,4a] In **1b** the Cu–N bonds are shorter, and the Cu–S bonds longer, than those reported for these copper(II) complexes;[3a,b] *i.e.* for n = 4, Cu–N 1.955(5) and Cu–S 2.221(2) Å.[3a] In the case of **2a** all Ni–L bonds are longer than for the cyclopentene-based nickel(II) complexes;[4a] for n = 4 Ni–N 1.919(4), 1.923(3) and Ni–S 2.162(1), 2.161(1) Å respectively.[4a]

NMR Spectra (see SUP 57187)

Scheme 1 shows the labelling used for the assignments. The ^{13}C NMR data for the zinc(II) complexes and for the protonated ligands, H_2L^1 and H_2L^2, are listed in Table 5. Room-temperature ^{1}H NMR spectra of the diamagnetic complexes are shown in Fig. 3. The temperature-dependent spectra of H_a and H_c for **2a** are plotted against 1/T in Fig. 4. For a planar complex only one resonance will be observed for each kind of proton listed in Scheme 1. For a complex that possesses pseudo-tetrahedral C_2 symmetry the H_a and H_b protons are diastereotopic, and two resonances will be observed for H_a and H_b, respectively. It is seen that the diamagnetic complexes and the nickel(II) complexes are all pseudo-tetrahedral and have C_2 symmetry

Table 4 Selected bond distances (Å) and angles (°) for complex **2a**

Ni–N(1)	1.932(2)	Ni–N(11)	1.935(2)
Ni–S(8)	2.196(1)	Ni–S(18)	2.187(1)
N(1)–C(2)	1.298(3)	N(11)–C(12)	1.295(3)
N(1)–C(23)	1.488(3)	N(11)–C(26)	1.484(4)
C(2)–C(3)	1.425(3)	C(12)–C(13)	1.416(4)
C(3)–C(4)	1.429(4)	C(13)–C(14)	1.425(4)
C(3)–C(7)	1.393(4)	C(13)–C(17)	1.401(4)
C(4)–N(5)	1.328(4)	C(14)–N(15)	1.325(4)
N(5)–N(6)	1.365(4)	N(15)–N(16)	1.367(3)
N(6)–C(7)	1.354(3)	N(16)–C(17)	1.341(4)
C(7)–S(8)	1.725(3)	C(17)–S(18)	1.723(3)
C(23)–C(24)	1.527(5)	C(25)–C(26)	1.526(5)
C(24)–C(25)	1.507(5)		
C(4)–C(30)	1.467(4)	C(14)–C(40)	1.474(4)
S(8)···S(18)	2.858(1)		
N(1)–Ni–N(11)	89.89(9)	S(8)–Ni–S(18)	81.40(3)
S(8)–Ni–N(11)	169.90(7)	N(1)–Ni–S(18)	169.51(7)
N(1)–Ni–S(8)	95.02(7)	N(11)–Ni–S(18)	95.22(7)
Ni–N(1)–C(2)	128.8(2)	Ni–N(11)–C(12)	128.5(2)
Ni–N(1)–C(23)	116.6(2)	Ni–N(11)–C(26)	117.5(2)
Ni–S(8)–C(7)	102.27(9)	Ni–S(18)–C(17)	102.68(9)
N(1)–C(2)–C(3)	124.6(3)	N(11)–C(12)–C(13)	125.2(2)
C(2)–C(3)–C(7)	123.3(3)	C(12)–C(13)–C(17)	123.4(2)
C(4)–C(3)–C(7)	105.3(2)	C(14)–C(13)–C(17)	104.7(2)
C(2)–C(3)–C(4)	130.6(3)	C(12)–C(13)–C(14)	131.2(2)
C(3)–C(4)–N(5)	110.4(3)	C(13)–C(14)–N(15)	110.9(2)
C(4)–N(5)–N(6)	105.6(2)	C(14)–N(15)–(16)	105.2(2)
N(5)–N(6)–C(7)	112.6(2)	N(15)–N(16)–C(17)	113.0(2)
C(3)–C(7)–N(6)	106.0(2)	C(13)–C(17)–N(16)	106.2(2)
N(6)–C(7)–S(8)	124.6(2)	N(16)–C(17)–S(18)	125.0(2)
C(3)–C(7)–S(8)	129.2(2)	C(13)–C(17)–S(18)	128.7(2)
C(2)–N(1)–C(23)	114.4(2)	C(12)–N(11)–C(26)	113.9(2)
N(1)–C(23)–C(24)	112.6(3)	N(11)–C(26)–C(25)	112.0(2)
C(23)–C(24)–C(25)	114.9(3)	C(24)–C(25)–C(26)	115.2(2)
N(1)–Ni–S(8) S(18)–Ni–N(11)	12.7(1)		
C(3)–C(4)–C(30)–C(31)	−157.3(4)		
C(3)–C(4)–C(30)–C(35)	23.9(5)		
N(5)–C(4)–C(30)–C(31)	24.1(5)		
N(5)–C(4)–C(30)–C(35)	−154.6(3)		
C(13)–C(14)–C(40)–C(41)	−152.1(3)		
C(13)–C(14)–C(40)–C(45)	28.8(5)		
N(15)–C(14)–C(40)–C(41)	28.8(5)		
N(15)–C(14)–C(40)–C(45)	−152.3(04)		

E.s.d.s of the least significant digits are in parentheses.

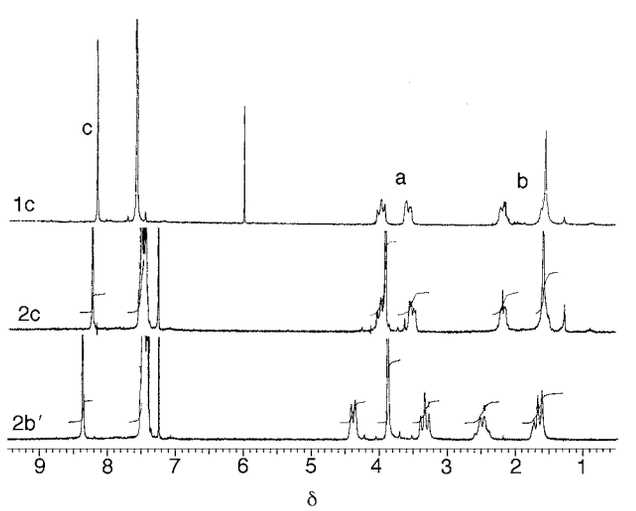

Fig. 3 The 200 MHz ^{1}H NMR spectra at 25 °C of complex **1c** in $CDCl_2CDCl_2$ and of **2c** and **2b**′ in $CDCl_3$

Table 5 Carbon-13 NMR data for complexes **1c** and **2c** and the protonated pro-ligands at 25 °C

Compound	a	b	c	d	e	f	Me	s	o	m	p
H_2L^1 [a]	50.06	26.88	158.1	195.2	105.2	161.8	—	127.3	128.8	129.4	130.6
1c [b]	59.37	31.18	162.0	181.8	108.7	162.7	—	126.6	128.4	128.8	130.1
H_2L^2 [c]	50.52	27.88	156.1	168.1	110.1	153.3	36.65	131.5	128.9	129.5	129.7
2c [c]	60.12	32.28	154.5	163.8	112.5	149.7	36.52	129.1	129.2	129.5	132.4

Chemical shifts are in ppm. [a] Measured in $(CD_3)_2SO$. [b] Measured in $CDCl_2CDCl_2$. [c] Measured in $CDCl_3$.

Table 6 Thermodynamic parameters for the spin-equilibrium process for complexes **1b** and **2a** in CD_2Cl_2 [a]

	Complex	
Parameter	**1a**	**2a**
ΔH/kJ mol^{-1}	13.6 ± 0.6	15.8 ± 0.3
ΔS/J K^{-1} mol^{-1}	35.0 ± 2.7	26.8 ± 1.1
ΔG_{25}/kJ mol^{-1}	3.2 ± 0.2	7.8 ± 0.1
Correlation coefficient [b]	0.9989	0.9997

[a] See Experimental section for the derivation of standard deviations. [b] Of the plot of ln K *vs.* $1/T$; K is 0.281 and 0.0430 at 25 °C for complexes **1a** and **2a**, respectively.

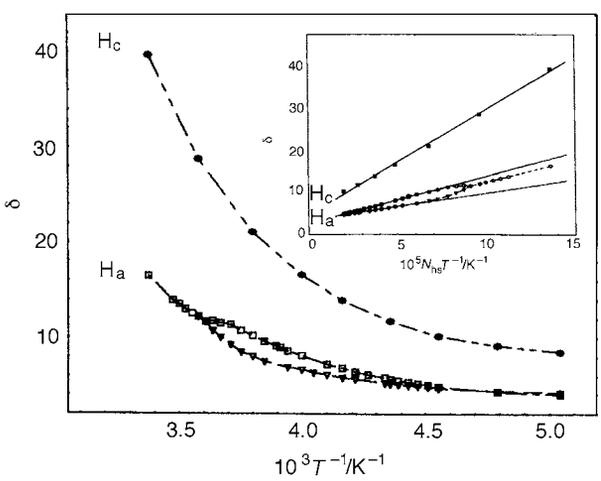

Fig. 4 Chemical shifts of H_a and H_c plotted against $1/T$ and (insert) against N_{hs}/T from the temperature-dependent 400 MHz ^{1}H NMR spectra of complex **2a** in CD_2Cl_2

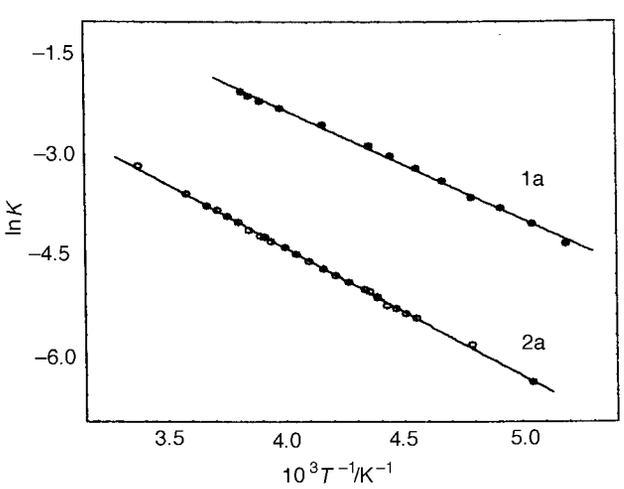

Fig. 5 Van't Hoff plots for the spin-equilibrium processes of complexes **1a** and **2a** in CD_2Cl_2

in solution. It has been shown by nuclear Overhauser effect spectroscopy (NOESY) experiments[6] that a zinc(II) complex similar to **1c** and **2c** is distorted towards a planar geometry in solution. The same is expected for the zinc(II) complexes investigated in this work. Pseudo-tetrahedral surroundings[2] are expected for

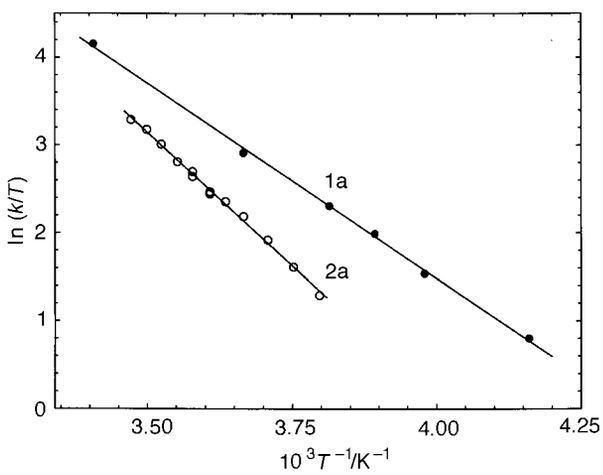

Fig. 6 Eyring plots for the racemization processes of complexes **1a** and **2a** in CD_2Cl_2

the copper(I) ions in **2b′**. The smaller $\Delta\nu$, the chemical shift difference between diastereotopic protons, for **1c** ($\Delta\nu_a = 74$, $\Delta\nu_b = 124$ Hz) and **2c** ($\Delta\nu_a = 92$, $\Delta\nu_b = 126$ Hz) compared with **2b′** ($\Delta\nu_a = 212$, $\Delta\nu_b = 164$ Hz) is probably indicative of a distortion towards a planar geometry and less deviant chemical surroundings for the diastereotopic protons of the zinc(II) complexes. Important differences between **1c** and **2c** are seen, however, in the ^{13}C NMR spectra, in particular for C_d. The downfield shift observed for H_2L^1 and **1c** compared with H_2L^2 and **2c** is probably due mainly to a large electron-withdrawing effect from the neighbouring oxygen atom in the isoxazole ring.

Not surprisingly the zinc(II) complexes do not racemize below 90 °C. The same configurational rigidity was observed previously for similar Schiff-base complexes,[6] whereas the racemization process is evident in complexes with more flexible bidentate ligands.[6]

Thermodynamic parameters for the spin-equilibrium process (see SUP 57187)

A non-Curie dependence for the isotropic shift is observed in the temperature-dependent ^{1}H NMR spectra of the nickel(II) complexes in CD_2Cl_2, see Fig. 4 for **2a**. This is indicative of a spin-equilibrium process $S = 0 \rightleftharpoons S = 1$. An estimated coupling constant, A_i, and the observed isotropic shifts for an indicator proton, H_i, were used to determine the equilibrium constants for the spin-equilibrium process,[7] see Experimental section. In Fig. 4 (insert) the observed shifts for protons other than the indicator proton H_i have been plotted against N_{hs}/T where N_{hs} is the mole fraction of high-spin molecules. Straight lines with correlations close to unity and non-zero intercepts $|B| < \approx 10$ ppm[8a] for strongly coupled protons confirm a reasonable estimate for the coupling constant A_i in the first step of the procedure. The van't Hoff plots are shown in Fig. 5, and the resulting thermodynamic parameters are listed in Table 6. They are in good agreement with the results obtained in chlorinated solvents for most other nickel(II) complexes with tetradentate N_2S_2 Schiff-base ligands[4a,b,d] (3.7–11.3 kJ mol^{-1} for ΔG at 25 °C). The values reported in ref. 4(*c*) for a system similar to **2a** measured in chloroform are unusually low.

Table 7 Kinetic parameters for the racemization process for complexes **1a** and **2a** in CD_2Cl_2[a]

Parameter	Complex **1a**	**2a**
$\Delta H^{\ddagger}$/kJ mol^{-1}	37.0 ± 1.4	50.3 ± 2.7
$\Delta S^{\ddagger}$/J K^{-1} mol^{-1}	−37.4 ± 5.1	5.5 ± 9.9
$\Delta G^{\ddagger}_{25}$/kJ mol^{-1}	48.2 ± 0.2	48.9 ± 0.2
Correlation coefficient[b]	0.9994	0.9981

[a] See Experimental section for the derivation of standard deviations. Activation parameters were derived from the Eyring equation: $k(T) = T(k_B/h)\exp(\Delta S^{\ddagger}/R)\exp(-\Delta H^{\ddagger}/RT)$; k_B is the Boltzmann constant. The rate constants were derived from the equations: $T \leqslant T_c$, $k(T) = 0.5\pi[2(\Delta\nu^{02} - \Delta\nu^2)]^{\frac{1}{2}}$;[10a] $T \geqslant T_c$, $k(T) = 0.5\pi\Delta\nu^0[(\Delta\nu^0/\nu_{\frac{1}{2}})^2 - (\nu_{\frac{1}{2}}/\Delta\nu^0)^2 + 2]^{\frac{1}{2}}$;[10b] T_c is the coalescence temperature, $\Delta\nu^0$ the chemical shift difference between the indicator protons in the absence of exchange. [b] Of the plot of ln (k/T) *vs.* $1/T$; $k = 2.3 \times 10^4$ and 1.7×10^4 s^{-1} at 25 °C for complexes **1a** and **2a**, respectively.

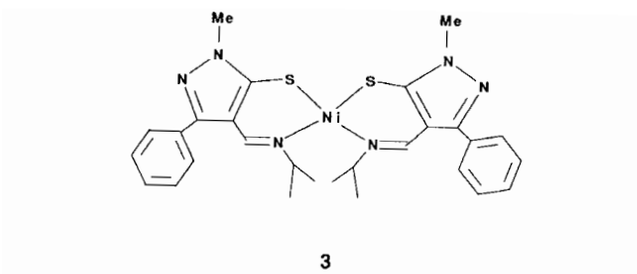

3

The value of ΔH is less positive for **1a** than for **2a**. However, the relatively large preference for the high-spin state, and for the associated pseudo-tetrahedral configuration, for **1a** is mainly entropy driven. The large value for ΔS in the case of **1a** is possibly attributed to a strong solvation of the planar low-spin form, as the bulkiness of the ligands is similar for the two systems. A stronger solvation of the metal centre should be in accord with the stronger Lewis acidity expected for the complexes **1a**–**1c** due to the electron-withdrawing effect from the isoxazole oxygen atom.[8b,c]

Kinetic parameters for the racemization process (see SUP 57187)

The procedure of ref. 9 was used with some modifications to obtain rate constants for the racemization process $\Delta \rightleftharpoons \Lambda$ for the nickel(II) complexes, see Experimental section. The Eyring plots are shown in Fig. 6 and the resulting activation parameters are listed in Table 7.

No concentration dependence of the racemization rate was found for complex **2a**, investigated in concentrations of 5 and 10 mg cm^{-3}. The concentration dependence was not examined for **1a** because of a very low solubility (3 mg cm^{-3}). The reaction mechanism is intramolecular for **2a**, and probably for **1a** also. A racemization mainly *via* a planar transition state without bond rupture is assumed.[6,9] The kinetic parameters for **1a** are consistent with a twist mechanism; $\Delta H^{\ddagger}$ and $\Delta S^{\ddagger}$ are 26.5 kJ mol^{-1} and −75.6 J K^{-1} mol^{-1}, respectively, for the bis(bidentate ligand)nickel(II) complex **3** measured in CD_2Cl_2.[9] As the isopropyl group is more bulky than the butylene chain, a racemization *via* a *cis* planar transition state is believed to produce the more negative $\Delta S^{\ddagger}$ for **3**. The less positive $\Delta H^{\ddagger}$ for **3** may be due to the larger flexibility of this fully paramagnetic system. Additionally, the observed differences between **1a** and **3** are in accordance with the assumption of a diamagnetic transition state,[11] as the M–L bond contraction should be strongest and the activation parameters $\Delta H^{\ddagger}$ and $\Delta S^{\ddagger}$ smallest for the more paramagnetic complex.

A strong solvation of a planar transition state is believed to reduce $\Delta S^{\ddagger}$ for complex **1a** compared with **2a** in accordance with the thermodynamic parameters for the spin-equilibrium

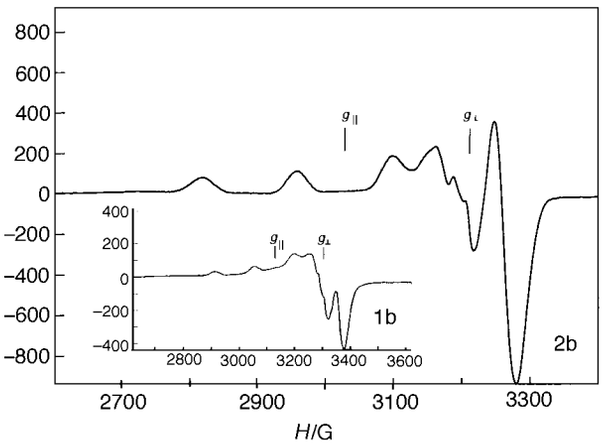

Fig. 7 The ESR spectra of complexes **1b** and **2b** at 120 K

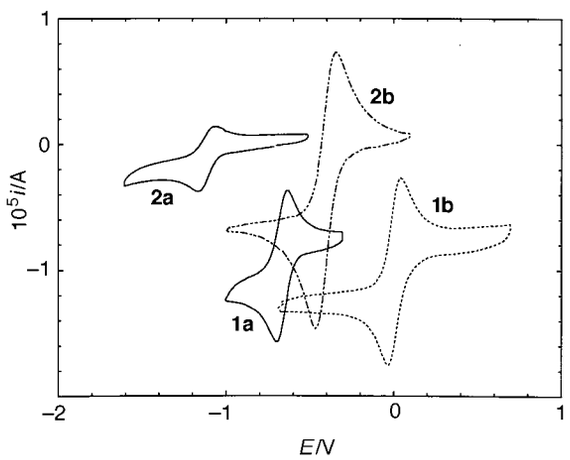

Fig. 8 Cyclic voltammograms of the nickel(II) and copper(II) complexes. Sweep rate 100 mV s^{-1}

process (see above). The large positive $\Delta H^{\ddagger}$ for **2a** and a $\Delta S^{\ddagger} \approx 0$, however, may indicate that the racemization for this complex takes place partly *via* a bond-rupture mechanism. The kinetic parameters found for a series of differently substituted nickel(II) analogues of **2a** are similar.[4d]

Electronic spectra

For the nickel(II) complexes (see Experimental section) the UV/VIS region is complicated due to the presence of low-spin molecules (D_{4h} symmetry is assumed) as well as high-spin molecules (T_d symmetry is assumed). By comparisons with the diamagnetic ethylene-bridged analogue of **2a*** and with the paramagnetic analogue **3**† it is seen that the low-spin population is dominant in accordance with the thermodynamic measurements. Owing to the resemblance with the zinc(II) spectra (see Experimental section) the high-energy bands at and below ≈350 nm are assigned to intraligand transitions. The shoulder at 485 (**1a**) and the band at 540 nm (**2a**) are assigned to a ligand-to-metal charge-transfer (l.m.c.t.) transition $S_{\pi} \rightarrow Ni$ derived from high-spin molecules, and the shoulder at 415 nm to a superposition of the l.m.c.t. transitions $S_{\sigma} \rightarrow Ni$ and $S_{\pi} \rightarrow Ni$ from the high- and low-spin forms, respectively. In the visible region the bands at 680 (**1a**) and at 655 nm (**2a**) are assigned to a superposition of $^3T_1$ (P) with the $^1A_{2g}$ transition derived from low-spin molecules. The origin of the transitions in the near-

* UV/VIS:[12a] 649 (110), 494 (sh) (155), 405 (sh) (2400), 380 (sh) (3710), 345 (sh) (12 260), 331 (13 410) and 286 nm (52 560 dm^3 mol^{-1} cm^{-1}).
† UV/VIS/NIR:[9] 1575 (33.6), 665 (448), 508 (3075), 400 (sh) (2310),[12b] 300 (23 100)[12b] and 250 (sh) nm (46 000 dm^3 mol^{-1} cm^{-1}).[12b]

Table 8 Electrochemical and spectroscopic data for the copper(II) complexes

	Reduction[a]		Electronic[b]			ESR					
Complex	$E_{\frac{1}{2}}$/mV	ΔE/mV	l.f. ^{2}E	c.t.		g_0	10^3A_0/cm^{-1}	$g_\parallel$	$g_\perp$[c]	$10^3A_\parallel$/cm^{-1}	$10^3A_\perp$[c]/cm^{-1}
1b	3	73	1153 (0.10)	640 (sh) (1.13)	527 (2.68)	2.078	5.62	2.155	2.040	14.22	1.3
2b	−407	120	1154 (0.10)	650 (1.28)	522 (2.81)	2.076	5.92	2.156	2.036	14.06	1.9
Azurin[14a]	230[d]			770 (0.26)	620 (10.5) 470 (1.3)			2.260	2.050	6	—
Azurin[13]			≈1000	780 (0.78)	630 (3.80) 570 (0.54)						

Parameters for Cu_A:[14b] E_m[14c] ≈ 260 mV; g(i) = 2.185 (z), 1.99 (x), 2.03 (y); A(i) = 3.0 (z), 2.0 (x), 2.5 (y). [a] Complexes **1b** and **2b** were measured in MeCN *vs.* Ag–AgCl. The listed ΔE values are for a sweep rate of 100 mV s^{-1}. [b] Energies of ligand-field (l.f.) and charge-transfer (c.t.) bands in nm, with 10^{-3}ε/dm^3 mol^{-1} cm^{-1} in parentheses. The assignment is for a D_{2d} symmetry.[13] The ground state is $^2B_2$. [c] For complexes **1b** and **2b** $g_\perp$ and $A_\perp$ have been calculated from the relations $g_0 = \frac{1}{3}(g_\parallel + 2g_\perp)$ and $A_0 = \frac{1}{3}(A_\parallel + 2A_\perp)$. [d] E_m.

infrared region are high-spin molecules only. The first band is assigned to a component of the $^3T_1$ (F) transition, split by the actual lower symmetry (pseudo-D_{2d}), the second to the $^3A_2$ (F) transition.

For the copper(II) complexes the intraligand transitions are easily identified by comparison with the analogous zinc(II) complexes (see Experimental section). The copper(II) and zinc(II) ions seem to distort the ligand in a similar manner. The spectra are simple in the near-infrared and visible regions, see Table 8. The ligand-field band is assigned to the ^{2}E transition in D_{2d} symmetry, the c.t. bands to the $S_\pi \rightarrow Cu$ and $S_\sigma \rightarrow Cu$ transitions.[13] With the exception of a slightly red-shifted $S_\sigma \rightarrow Cu$ transition for **1b** compared with **2b** the spectra are almost identical. The spectrum of azurin is listed in Table 8 for comparison. That of plastocyanin is similar.[13]

ESR spectra

The ESR parameters for the copper(II) complexes are listed in Table 8. The spectra measured in $CHCl_3$–toluene at 120 K are in Fig. 7. They are typical for molecules of pseudo-axial symmetry having $g_z \gg g_x \approx g_y$. The powder spectrum of **1b** doped into the analogous zinc(II) complex is no different. The parameters are almost identical for the two complexes, and similar to those for other tetrahedrally distorted $n = 4$ complexes with sulfur-containing ligands.[3a,c,d,15a] An increased distortion from a planar geometry with increasing n is reflected in the large g values and small A values; $g_\parallel = 2.139$ and $A_\parallel = 18.4 \times 10^{-3}$ cm^{-1} were reported[15b] for a $n = 2$ pyrazolyl dimethyl substituted complex similar to **2b**. This is probably the normal trend.[3b,15a] The ESR parameters for azurin and for the binuclear Cu_A site of cytochrome c oxidase are listed in Table 8 for comparison.

Electrochemistry

The cyclic voltammograms of nickel(II) and copper(II) complexes measured in MeCN *vs.* Ag–AgCl are shown in Fig. 8, and the electrochemical data for **1b** and **2c** are listed in Table 8. The M^{II}–M^{III} oxidation peaks are obscured by peaks due to ligand oxidation.[6] In a series of pyrazole-containing nickel(II) N_2S_2 complexes similar to **2a** the half-wave potential is more than 1 V.[4d] For the Ni^{II}–Ni^{I} reduction the half-wave potentials are −667 and −1112 mV for **1a** and **2a**, respectively. The corresponding separations between the reduction and oxidation peaks are 60 and 91 mV for a sweep rate of 100 mV s^{-1}. The M^{II}–M^{I} reductions are quasi-reversible in every case. In spite of the almost identical spectral properties observed especially for the copper(II) complexes, the ligand H_2L^1 is much more reducing than H_2L^2, and more reducing than several other tetradentate N_2S_2 Schiff-base ligands containing cyclopentene or pyrazole and bridged by four carbon atoms.[3b,d,4a,d] The electrochemistry is closer to that of the N_2S_2 Schiff-base complexes incorporating pyridinium[16a] or which have a N_2S_2 thioether donor set.[16b,c] A half-wave potential of 200 mV has been reported for the $n = 4$ pyridinium-containing complex.[16a] Electrochemical parameters for azurin and for the Cu_A site of cytochrome c oxidase are listed in Table 8 for comparison.

Conclusion

The complexes investigated are insoluble in water, and all measurements have been performed in organic solvents. Consequently, too rigorous comparisons with the metalloenzymes should be avoided. Some tendencies may be evaluated, though. It is known that the present zinc(II) complexes are not suitable models for the zinc-containing alcohol dehydrogenases,[6] and it is seen in this work and in ref. 4(*d*) that the nickel(II) complexes are not suitable models for the nickel-containing hydrogenases which have unusually low redox potentials for the Ni^{II}–Ni^{III} oxidation ($E_0 < 0$).[17] In this work the complexes of Ni^{II} and Zn^{II} have served as valuable contributors of information, *e.g.* about the influence of the co-ordinated metal on the ligand (Zn^{II}), and about the relative preferences for a pseudo-tetrahedral geometry in solution (Ni^{II}).

The spectral properties of the copper(II) complexes and the electrochemical properties of **2b** are very different from those of the blue copper enzymes. A modified version of **1b**, however, may be a suitable model for the latter due to the high potential for the Cu^{II}–Cu^{I} reduction. The main reason for the high potential is probably an electron-withdrawing effect from the isoxazole oxygen. This is supposed (1) to reduce the electron–electron repulsion on the copper ion, and (2) to lower the Lewis basicity of the sulfur donor atom, thus producing a weaker ligand field and a distortion from a planar co-ordination geometry.

In spite of rather similar co-ordination geometries, according to the spectral properties, the potential for the copper(II) reduction of the $n = 4$ N_2S_2 Schiff-base complexes with thiolate-sulfur donor atoms increases in the same order as the expected electron-withdrawing effect from the incorporated ring: cyclopentene[3b] < pyrazole < isoxazole < pyridinium.[16a]

The potential for the copper(II) reduction seems to be inversely correlated with the Lewis basicity of the sulfur donor atoms. The potential increases, and, according to the Cu–S bond lengths in the solid state for some copper(II) Schiff-base complexes, the Lewis basicity decreases in the order: $n = 4$, cyclopentene, $(NS)_2$[3a] ≥ $n = 4$, pyrazole, $(NS)_2$[3c,d] > $n = 4$, isoxazole, $(NS)_2$ ≥ $n = 3$, pyridinium, $(NS)_2$[16a] ≫ bis-bidentate or tetradentate thioether complexes, $(NSR)_2$.[16b,c] The copper(II) thioether complexes are six-[16b] or five-co-ordinate.[16c] For the four-co-ordinate complexes the relative preference for a tetra-

hedrally distorted co-ordination geometry is probably important, as tetrahedral surroundings are preferred by the d^{10} ion Cu^{I}. For complexes with the same type of ligands the potential for the copper(II) reduction is highest in the most tetrahedrally distorted complex.[3b,16a] A relatively high preference for the pseudo-tetrahedral geometry for **1b** may be part of the explanation for the high reduction potential.

Experimental

Materials

Chemicals for the preparations were reagent grade and commercially available, used as received. Solvents used for analytical purposes were spectroscopic grade. Acetonitrile used for cyclic voltammetry and $CHCl_3$ for UV/VIS/NIR spectroscopy were boiled over phosphorus pentaoxide and distilled immediately before use.

Preparation

Protonated pro-ligands. The appropriate *o*-chloroaldehyde used as starting material was prepared according to ref. 18. For 2-chloro-3-formylisoxazole (yield 67.8%) a slightly modified procedure was used: the reaction of 3-phenylisoxazol-5-one with the Vielsmayer reagent was performed over 4 d at 45 °C. Compounds H_2L^1 and H_2L^2 were prepared according to ref. 6. UV: H_2L^1, 382 (10 040) and 265 (sh) (12 540); H_2L^2, 399 (8230) and 304 nm (20 920 dm^{-3} mol^{-1} cm^{-1}).

Complexes. *Nickel*(II). To a suspension of protonated pro-ligand (0.2 mmol) in methanol (3 cm^3) was added nickel(II) acetate tetrahydrate (0.2 mmol). The mixture was stirred at room temperature for 4 h. The dark green complex was filtered off and washed with MeOH on the filter. The complexes were recrystallized from CH_2Cl_2 (**1a**) or $CHCl_3$ (**2a**). They are green and diamagnetic in the solid state at room temperature ($\mu_{eff} \approx 1$ μ_B at 22 °C) and in solution at low temperature, red and paramagnetic in solution at elevated temperatures.

UV/VIS/NIR: **1a**, ≈1700 (13.8), 1220 (16.7), 680 (215), 485 (sh) (850), 415 (sh) (2085), 350 (sh) (6211) and 296 (20 650); **2a**, ≈1775 (3.6), 1225 (5.4), 655 (205), 540 (295), 415 (sh) (2000), 355 (sh) (7390) and 295 nm (43 000 dm^3 mol^{-1} cm^{-1}).

To a suspension of H_2L^1 (0.2 mmol) in absolute EtOH (10 cm^3) was added copper(II) acetate dihydrate (0.2 mmol) in absolute EtOH (5 cm^3). The mixture was stirred at reflux temperature for 20 min. The dark violet complex **1b** was filtered off and washed with MeOH on the filter. UV: intraligand bands at 370 (sh) (6780), 342 (13 450) and 253 (sh) nm (23 550 dm^3 mol^{-1} cm^{-1}).

To a suspension of H_2L^2 (0.2 mmol) in MeOH (10 cm^3) was added copper(II) acetate dihydrate (0.2 mmol) in MeOH (5 cm^3). The mixture was stirred at room temperature for 1 h. The dark brownish green complex **2b** was filtered off and washed with MeOH on the filter. It is purple in solution. UV: intraligand bands at 346 (22 500), 296 (41 000) and 264 nm (41 500 dm^3 mol^{-1} cm^{-1}).

To a suspension of H_2L^1 (0.2 mmol) in absolute EtOH (10 cm^3) was added copper(II) acetate dihydrate (0.4 mmol) in absolute EtOH (5 cm^3). The mixture was stirred for 3.5 h at room temperature. The yellow complex **2b′** was filtered off and washed with MeOH on the filter. It is pale yellow in solution.

To a suspension of H_2L^1 (0.2 mmol) in MeCN (5 cm^3) was added zinc(II) acetate dihydrate (0.2 mmol) and Na (5 mg) in MeOH (3 cm^3). The mixture was stirred at reflux temperature for 1 h. The pale yellow complex **1c** was filtered off and washed with MeOH on the filter. It is pale yellow in solution. UV: 355 (sh) (15 000), 342 (16 910) and 255 (sh) nm (31 760 dm^3 mol^{-1} cm^{-1}).

To a suspension of H_2L^2 in MeOH was added zinc(II) acetate dihydrate (0.2 mmol) and Na (5 mg) in MeOH (3 cm^3). The mixture was stirred at reflux temperature for 0.5 h. The almost white complex **2c** was filtered off and washed with MeOH on the filter. It is pale yellow in solution. UV: 336 (12 080), 289 (27 130) and 265 (sh) nm (31 450 dm^3 mol^{-1} cm^{-1}).

Physical measurements

Proton and ^{13}C NMR spectra of pro-ligands and complexes (3–15 mg cm^{-3}) were obtained on Varian spectrometers (Gemini 200 and Unity 400 MHz) in $CDCl_3$ or $(CD_3)_2SO$. Methanol was used for temperature calibration at low temperature, ethylene glycol at high temperature. The uncertainty of the temperature was 1°. Assignments for ligands and complexes were accomplished by comparisons between the systems, selective decoupling of single protons and attached proton test spectroscopy. The ESR spectra of the copper(II) complexes in $CHCl_3$–toluene or as Cu/Zn powders were obtained at room temperature and at −153 °C on a 9 GHz Bruker (ESP 300E) instrument. Electrochemical data were collected in MeCN under nitrogen by cyclic voltammetry. Conditions: room temperature; 3–4 mmol dm^{-3} copper(II) complexes, 1–2 mmol dm^{-3} nickel(II) complexes; sweep rate, 50–300 mV s^{-1}; microelectrodes from BAS100; platinum working and counter electrodes and an Ag–AgCl (water-based) reference electrode; supporting electrolyte, 0.1 mol dm^{-3} tetrabutylammonium hexafluorophosphate; external standard, ferrocene ($E_{\frac{1}{2}} = 0.500$ V under the given conditions). The electrolyte and the investigated compounds were dried in vacuum before use. The solvent with NBu_4PF_6 was scanned before use to check the purity of the solvent. Electronic absorption spectra were obtained in $CHCl_3$ at 20 °C in a 1 cm quartz cuvette on a thermostatted Shimadzu UV-3100 apparatus, electron impact mass spectra on a Finnigan Mat SSQ710 or a Varian Mat 311A apparatus and FAB mass spectra (in $CHCl_3$) on a Kratos MS 50RF apparatus. Magnetic susceptibilities of the nickel(II) complexes in the solid state were measured at 22 °C on a Sherwood Scientific magnetic susceptibility balance.[18] Diamagnetic corrections were made using Pascal's constants. Elemental analyses were performed at the H. C. Ørsted Institute, University of Copenhagen. The complexes were first dried in vacuum.

Thermodynamic parameters for the spin-equilibrium process

Equilibrium constants, $K(T)$, were evaluated from the temperature-dependent ^1H NMR spectra in the ranges −80 to −10 and −75 to 23 °C for complexes **1a** and **2a**, respectively, using equation (1) for the paramagnetic isotropic Fermi-

$$\delta_{i,obs} = -[A_i N_{hs} \gamma_e h S(S+1) 10^6 / 3\gamma_H kT] + \delta_{i,dia}{}^7 \qquad (1)$$

contact shift for H_i, in the form presented in ref. 9. The coupling constant A_i is in units of Hz (1 G = 2.8 MHz), $\delta_{i,obs}$ is the observed shift (in ppm), $\delta_{i,dia}$ the shift of the diamagnetic reference (in ppm); the other symbols have their usual meanings. The substitution of a known coupling constant for A_i yields N_{hs} and $K = N_{hs}/(1 - N_{hs})$. The values $A_m = 0.0118$ G (for **1a**) and $A_{Me} = 0.0382$ G (for **2a**) found[9] for the paramagnetic nickel(II) complex **3** were used. The diamagnetic references are the chemical shift at −100 °C found by linear extrapolation from plots of $\delta_{i,obs}$ *vs.* T at the lowest measuring temperatures.

Kinetic parameters for the racemization process

Rate constants were obtained from the temperature-dependent ^1H NMR spectra of exchanging protons by the method used for paramagnetic nickel(II) complexes[9] with modifications necessary for the spin-equilibrium systems investigated in this work. Corrections for $\Delta\nu°(T)$, the natural chemical shift difference between the resonances for exchanging protons, were obtained by linear extrapolation from plots of $\Delta\delta°(T)$, collected in the

stopped-exchange temperature range, *vs.* N_{hs}/T. The natural linewidths of the resonances for exchanging protons, $\nu_{\frac{1}{2}}^{\circ}(T)$, were evaluated from the linewidths for other protons in the molecule.

Statistics

The uncertainties of the thermodynamic and kinetic parameters (Tables 6 and 7) were evaluated from the standard errors (s.e.s) of the linear plots s.e. $= [\Sigma(y_i - y_i')^2/(n-2)]^{\frac{1}{2}}$ where $y_i - y_i'$ is the vertical distance between the regression line and an arbitrary measuring point. The maximum and minimum slopes (yielding ΔH_{max}, ΔH_{min} and $\Delta H^{\ddagger}_{max}$, $\Delta H^{\ddagger}_{min}$) and intercepts (yielding ΔS_{max}, ΔS_{min} and $\Delta S^{\ddagger}_{max}$, $\Delta S^{\ddagger}_{min}$) were found from the lines between two of the four points (x_i, $y_i' \pm$ s.e.) plotted at the highest and lowest measuring temperatures, $1/x_i$.[19] The s.d.s were evaluated from the maximum and minimum values of the parameters.

Crystallography

Dark violet (**1b**) and dark green (**2a**) crystals were grown from MeCN–CH_2Cl_2 (1:1). The crystals were mounted on a Huber diffractometer, and the cell parameters determined from the setting angles measured with graphite-monochromatized Mo-Kα radiation (λ 0.710 73 Å). For complex **1b** 36 reflections with a 2θ range of 16.6–26.2° were measured at ±2θ, for **2a** 30 reflections with 2θ 20.2–25.8° were measured at ±2θ and at high and low χ. Intensities were measured at room temperature (21 °C) using ω–2θ scans. Two standard reflections were measured every 50. Data were corrected for background, Lorentz-polarization effects and decay. An empirical absorption correction [20a] was applied for **1b** whereas that for **2a** was by integration. The structures were determined by direct methods, using SIR 92 [20b] for **1b** and SHELXS 86 [20c] for **2a** and refined by least-squares minimization of $\Sigma w(|F_o| - |F_c|)^2$ using a modification of ORFLS.[20d] All non-hydrogen atoms were refined anisotropically whilst hydrogen atoms were refined isotropically. Scattering factors and anomalous dispersion corrections for Ni and Cu were taken from ref. 20(*e*). Details are given in Table 2.

Atomic coordinates, thermal parameters, and bond lengths and angles have been deposited at the Cambridge Crystallographic Data Centre (CCDC). See Instructions for Authors, *J. Chem. Soc., Dalton Trans.*, 1997, Issue 1. Any request to the CCDC for this material should quote the full literature citation and the reference number 186/271.

Acknowledgements

The authors gratefully acknowledge Mrs. B. Heinrich and Mrs. T. Meinel, Leipzig University (L.U.), and Mrs. I. Pedersen and Mr. O. T. Sørensen, Odense University (O.U.), for technical assistance, Dr. L. Hennig (L.U.), Professor R. Kirmse (L.U.) and Professor H. Toftlund (O.U.) for providing laboratory facilities (to A. l. C.) and the Danish Natural Science Research Council and the Carlsberg Foundation for the diffractometer (to A. H. and R. H.).

References

1 H. Eklund, B. Nordström, E. Zeppezauer, G. Söderlund, I. Ohlsson, T. Boiwe, B.-O. Söderberg, O. Tapia, C.-I. Bränden and Å. Åkeson, *J. Mol. Biol.*, 1976, **102**, 27; A. Volbeda, M.-H. Charon, C. Piras, E. C. Hatchikian, M. Frey and J. C. Fontecilla-Camps, *Nature* (*London*), 1995, **373**, 580; T. Tsukihara, H. Aoyama, E. Yamashita, T. Tomizaki, H. Yamaguchi, K. Shinzawa-Itoh, R. Nakashima, R. Yaono and S. Yoshikawa, *Science*, 1995, **269**, 1069; E. T. Adam, R. E. Stenkamp, L. C. Sieker and L. H. Jensen, *J. Mol. Biol.*, 1978, **123**, 35; P. M. Colman, H. C. Freeman, J. M. Guss, M. Murata, V. A. Norris, J. A. M. Ramshaw and M. P. Verkatapa, *Nature* (*London*), 1978, **272**, 319.

2 J. C. Rasmussen, H. Toftlund, A. N. Nivorozhkin, J. Bourassa and P. C. Ford, *Inorg. Chim. Acta*, in the press.

3 (*a*) R. D. Bereman, G. D. Shields, J. Bordner and J. R. Dorfman, *Inorg. Chem.*, 1981, **20**, 2165; (*b*) R. D. Bereman, J. R. Dorfman, J. Bordner, D. P. Rillema, P. McCarthy and G. D. Shields, *J. Inorg. Biochem.*, 1982, **16**, 47; (*c*) O. P. Anderson, J. Becher, H. Frydendahl, L. F. Taylor and H. Toftlund, *J. Chem. Soc., Chem. Commun.*, 1986, 699; (*d*) L. Hennig, R. Kirmse, O. Hammerich, S. Larsen, H. Frydendahl, H. Toftlund and J. Becher, *Inorg. Chim. Acta*, 1995, **234**, 67.

4 (*a*) E. M. Martin, R. D. Bereman and P. Singh, *Inorg. Chem.*, 1991, **30**, 957; (*b*) H. Frydendahl, H. Toftlund, J. Becher, J. C. Dutton, K. S. Murray, L. F. Taylor, O. P. Anderson and E. R. T. Tiekink, *Inorg. Chem.*, 1995, **34**, 4467; (*c*) A. L. Nivorozhkin, L. E. Konstantinovsky, L. E. Nivorozhkin, V. I. Minkin, T. G. Takhirov, O. A. Diachenko and D. B. Tagiev, *Izv. Akad. Nauk. SSSR, Ser. Khim.*, 1990, 327 (in Russian); (*d*) A. la Cour, M. Findeisen, C. E. Olsen and O. Simonsen, unpublished work.

5 T. L. Gilchrist, *Heterocyclic Chemistry*, Wiley, New York, 1987, pp. 12–14.

6 O. P. Anderson, A. la Cour, M. Findeisen, L. Hennig, O. Simonsen, L. F. Taylor and H. Toftlund, preceding paper.

7 R. H. Holm, *Acc. Chem. Res.*, 1969, **2**, 307.

8 (*a*) W. D. Perry and R. S. Drago, *J. Am. Chem. Soc*, 1971, **93**, 2183; (*b*) A. Taha, V. Gutmann and W. Linert, *Monatsh. Chem.*, 1991, **122**, 327; (*c*) A. la Cour, M. Findeisen, R. Hazell, L. Hennig, C. E. Olsen and O. Simonsen, *J. Chem. Soc., Dalton Trans.*, 1996, 3437.

9 A. la Cour, B. Adhikhari, H. Toftlund and A. Hazell, *Inorg. Chim. Acta*, 1992, **202**, 145 and refs. therein.

10 (*a*) H. S. Gutowsky and C. H. Holm, *J. Chem. Phys.*, 1956, **25**, 1228; (*b*) A. Allerhand, H. S. Gutowsky, J. Jonas and R. A. Meinzer, *J. Am. Chem. Soc.*, 1966, **88**, 3185.

11 A. L. Nivorozhkin, M. S. Korobov, L. E. Konstantinovskii, L. E. Nivorozhkin and V. I. Minkin, *J. Gen. Chem. USSR*, 1985, 757.

12 (*a*) B. Adhikhari, A. la Cour, R. Hazell, C. E. Olsen and H. Toftlund, unpublished work; (*b*) A. la Cour, unpublished work.

13 A. B. P. Lever, *Inorganic Electronic Spectroscopy*, 2nd edn., Elsevier, Amsterdam, 1984, pp. 680–686.

14 (*a*) J. S. Fee, *Struct. Bonding* (*Berlin*), 1975, **23**, 1; (*b*) F. T. Greenaway, S. H. P. Chan and G. Vincow, *Biochem. Biophys. Acta*, 1977, **490**, 62; (*c*) R. W. Hay, *Bioinorganic Chemistry*, Ellis Horwood, Chichester, 1987, pp. 131–133.

15 (*a*) L. Casella, M. Gullotti and R. Vigano, *Inorg. Chim. Acta*, 1986, **124**, 121; (*b*) J. Becher, H. Toftlund, P. H. Olesen and H. Nissen, *Inorg. Chim. Acta*, 1985, **103**, 167.

16 (*a*) M. Gullotti, L. Casella, A. Pintar, E. Suardi, P. Zanello and S. Mangani, *J. Chem. Soc., Dalton Trans.*, 1989, 1979; (*b*) A. W. Addison, T. N. Rao and E. Sinn, *Inorg. Chem.*, 1984, **23**, 1957; (*c*) D. A. Nation, M. R. Taylor and K. P. Wainwright, *J. Chem. Soc., Dalton Trans.*, 1992, 1557.

17 J.-J. Krüger, G. Peng and R. H. Holm, *Inorg. Chem.*, 1991, **30**, 734 and refs therein.

18 J. Becher, P. H. Olesen, N. A. Knudsen and H. Toftlund, *Sulfur Lett.*, 1986, **4**, 175.

19 E. Winstrøm-Olsen, *Elementaer Usikkerhedsberegning* (Elementary Uncertainty Calculations), Akademisk Forlag, Copenhagen, 1974, pp. 33–35 (in Danish).

20 (*a*) S. Parkin, B. Moezzi and H. Hope, *J. Appl. Crystallogr.*, 1995, **28**, 53; (*b*) A. Altomare, G. Cascarano, C. Giacovazzo, A. Guagliardi, M. C. Burla, G. Polidori and M. Camalli, *J. Appl. Crystallogr.*, 1994, **27**, 435; (*c*) G. M. Sheldrick, SHELXS 86, Program for the Solution of Crystal Structures, 1986, University of Göttingen; (*d*) W. T. Busing, K. O. Martin and H. A. Levy, ORFLS, Report ORNL-TM-305, Oak Ridge National Laboratory, Oak Ridge, TN, 1962; (*e*) *International Tables for X-Ray Crystallography*, Kynoch Press, Birmingham, 1974, vol. 4, pp. 72–98.

Received 1*st April* 1996; *Paper* 6/02281B